

Chlorofluoriodomethane as a potential candidate for parity violation measurements

Pascale Soulard,^a Pierre Asselin,^a Arnaud Cuisset,^b Juan Ramon Aviles Moreno,^b Thérèse R. Huet,^b Denis Petitprez,^b Jean Demaison,^b Teresa B. Freedman,^c Xiaolin Cao,^c Laurence A. Nafie^c and Jeanne Crassous^{*d}

Received 26th July 2005, Accepted 11th October 2005

First published as an Advance Article on the web 21st November 2005

DOI: 10.1039/b510675c

CHFCII is among the more favorable molecules for parity violation (PV) measurements in molecules. Despite the fact that calculated PV effects are two orders of magnitude smaller than in some organometallic compounds, CHFCII displays interesting features which could make possible a new experimental PV test on this molecule. Indeed, ultrahigh resolution spectroscopy using an ultrastable CO₂ laser is favored by several intrinsic properties of this molecule. For example, the high vapor pressure of CHFCII allows investigation by supersonic beam spectroscopy. Indeed, the spectroscopic constants have been accurately determined by microwave and millimetre wave spectroscopy. This is important for the subsequent selection of an appropriate absorption band of CHFCII that could be brought to coincide with the absorption of CO₂. Partially resolved (+)- and (−)-CHFCII enantiomers with respectively 63.3 and 20.5% ee's have been recently prepared and analyzed by molecular recognition using chiral hosts called cryptophanes. Finally, the *S*-(+)/*R*-(−) absolute configuration was ascertained by vibrational circular dichroism (VCD) in the gas phase.

Introduction

Among the four fundamental forces that rule the physical world, the weak force is responsible for symmetry breaking in chiral molecules and leads to different energies for the two enantiomers.¹ To date, this energy difference due to parity violation, ΔE_{PV} , has never been clearly experimentally observed in molecules.² One of the possibilities to detect such a tiny effect (about 10^{-17} *kT* at room temperature) would be to measure differences in the frequencies of absorption bands, from the infra-red (IR) spectra of the two enantiomers.³ Such a test has already been done in the past, first by Arimondo *et al.* with camphor⁴ then by Chardonnet *et al.* with bromochlorofluoromethane.⁵ Although parity violation was not observed, the latter gave an upper limit of $\Delta E_{PV}/E = 10^{-13}$ for this effect.⁶ Contemporary with these experiments, very accurate DFT calculations including relativistic effects have predicted that PV in chiral molecules such as chiral fluorodiheterohalogenomethanes should exhibit differences between the two enantiomers in the C–F stretching band frequency up to 50 mHz when containing iodine (CHFCII

and CHFBrI).⁷ Consequently, chlorofluoriodomethane has appeared to be one favorable candidate for searching for parity violation effects. More recently, relative to the fact that the PV contribution is predicted to be proportional to Z^5 ,⁸ bigger molecules have been investigated with the same DFT methods by Schwerdtfeger and Bast.⁹ Parity violation effects of the order of 1 Hz have been calculated for several organometallic compounds containing an Os=O or a Re=O double bond,⁹ indicating that such transition metal complexes could be also good candidates for a PV experiment. Conversely, the high resolution spectroscopy of these molecules will not be a trivial issue.

Although the synthesis of the racemic form was achieved by Hazeldine *et al.* in 1952¹⁰ and later on by Novak *et al.*,¹¹ very little was known about chlorofluoriodomethane before the last two years. CHFCII is a small pentaatomic chiral molecule and as such it is an ideal model for theoretical studies. It has been possible to prepare the (+) and (−) enantiomers. Moreover Fourier transform infrared spectra in a supersonic beam for the racemic (\pm)-**1** have been recorded. First of all, microwave spectroscopy enables determination of accurate spectroscopic constants for the ground vibrational state and the rovibrational spectrum of the C–F stretching band could be experimentally obtained and roughly analyzed. The latter has revealed many bands that coincide with the ultrastable CO₂ laser which is currently used in Chardonnet's laboratory,⁵ and whose frequency variation does not exceed typically about 10^{-15} over a period of 24 h and is one of the key elements for obtaining high accuracy in experimental PV measurements, together with the use of jet cooling. Indeed, besides the ultrastable CO₂ laser, molecular beam spectroscopy using a

^a Université Pierre et Marie Curie-Paris 6, CNRS Laboratoire Dynamique Interactions et Réactivité, UMR 7075, Case 49, Place Jussieu, 75252 Paris Cedex 05, France

^b Laboratoire de Physique des Lasers, Atomes et Molécules (PhLAM), UMR 8523 CNRS-Université de Lille 1, 59655 Villeneuve d'Ascq Cedex, France

^c Department of Chemistry, Syracuse University, Syracuse, New York

^d Laboratoire de Chimie, École Normale Supérieure de Lyon, UMR CNRS 5182, 46, Allée d'Italie, F-69364 Lyon 07, France.

E-mail: jeanne.crassous@ens-lyon.fr

Fax: +33 04 72 72 84 83; Tel: +33 04 72 72 83 95

have been observed in the spectra for the two isotopomers. Here μ_a , μ_b and μ_c are the components of the total permanent electric dipole moment along the principal axes of inertia of the molecule. Moreover each rotational energy level is split into several sub-levels due to the interaction between the electric field gradient and the nuclear quadrupole moment of the iodine and chlorine nuclei giving an extremely complicated hyperfine pattern. Finally the presence of the two isotopomers ($\text{CHF}^{35}\text{ClI} = 75.8\%$ and $\text{CHF}^{37}\text{ClI} = 24.2\%$) adds difficulties for the identification of the spectra. All the observed components within the sensitivity of the spectrometer (328 for $\text{CHF}^{35}\text{ClI}$ and 140 for $\text{CHF}^{37}\text{ClI}$) were assigned in the 6–20 GHz frequency range. In the millimetre wave region only transitions (281 for $\text{CHF}^{35}\text{ClI}$) with relevant $J_{K_a K_c}$ quantum numbers were assigned in order to determine accurate centrifugal distortion constants. No hot lines were observed. The predicted rotational constants of the $\text{CHF}^{37}\text{ClI}$ were derived from the calculated *ab initio* structure of the $\text{CHF}^{35}\text{ClI}$ isotopologue (see the *ab initio* calculation section) for which the chlorine atom was given the appropriate mass. It is supposed that the equilibrium structure is isotopically invariant.

Due to the high resolution of the experimental techniques the analysis yielded accurate rotational and centrifugal distortion constants, the complete quadrupole coupling tensors for the iodine and chlorine nuclei, as well as the contribution of iodine to the spin–rotation interaction. These molecular parameters were determined for the two isotopomers $\text{CHF}^{35}\text{ClI}$ and $\text{CHF}^{37}\text{ClI}$. They reproduce the observed transitions within the experimental accuracy.

Effective Hamiltonian. The spectrum observed in the ground vibrational state of the singlet ground electronic state was analysed with a Hamiltonian model containing the molecular rotation and the associated centrifugal correction terms, the nuclear quadrupole interaction effect for the iodine and chlorine nuclei, and the nuclear spin–rotation interaction associated with the iodine atom:

$$\hat{H} = \hat{H}_R + \hat{H}_Q^{(I)} + \hat{H}_Q^{(Cl)} + \hat{H}_{CD} + \hat{H}_{NSR}^{(I)} \quad (1)$$

In eqn (1), the five terms are ordered according to the magnitude of their energetic contributions. The rigid asymmetric rotor Hamiltonian H_R is written as¹⁵

$$\hat{H}_R = \left[A - \frac{1}{2}(B+C) \right] \hat{J}_z^2 + (B+C) \hat{J}^2 + \frac{1}{2}(B-C) (\hat{J}_x^2 - \hat{J}_y^2) \quad (2)$$

with $\hat{J}^2 = \hat{J}_x^2 + \hat{J}_y^2 + \hat{J}_z^2$. The *I* prolate representation was used, and A , B and C are the principal rotational constants. H_{CD} denotes the centrifugal distortion terms of the Watson's A-reduced expression.¹⁶

The two-nuclear quadrupole interaction H_Q terms are written as¹⁶

$$\hat{H}_Q^{(N)} = \frac{1}{6} \sum_{i,j=x,y,z} \hat{Q}_{ij}^{(N)} \hat{V}_{ij}^{(N)}, \quad N = \text{I or Cl} \quad (3)$$

Eqn (3) describes the interaction between the nuclear quadrupole electric moment $Q^{(N)}$ and the molecular electric field gradient $V^{(N)}$ for the nucleus N . The spectroscopic parameters

are the elements of the quadrupole coupling tensor given by:

$$\chi_{\alpha\beta}^{(N)} = eQ^{(N)} \frac{\partial^2 V^{(N)}}{\partial \alpha \partial \beta} \quad (4)$$

α and β refer to the coordinates a , b , and c of the principal axes of inertia and e denotes the elementary charge. Only five parameters can be determined, that is two diagonal elements and three off-diagonal elements, associated with the real symmetric traceless quadrupole coupling tensor. In the case of CHClFI , the five parameters must be determined to account for the observed structure. Finally, the observed hyperfine structure revealed a contribution from the nuclear spin–rotation interaction. The Hamiltonian term H_{NSR} is written as in ref. 16 and 17 where the determined parameters are the elements of the second rank Cartesian tensor, C_{ij} , describing the spin–rotation coupling.

The observed microwave spectrum was analyzed using the Pickett's program.¹⁸ In CHClFI , the quadrupole interaction effect from the iodine nucleus ($Q^{(I)} = -0.710(10)$ b,¹⁹) is larger than that for the chlorine nucleus ($Q^{(35\text{Cl})} = -0.08165(80)$ b, $Q^{(37\text{Cl})} = -0.06435(64)$ b,²⁰) by almost one order of magnitude. Consequently we used the so-called sequential scheme for the addition of the angular momenta:

$$\begin{aligned} \hat{J} + \hat{I}_I &= \hat{F}_I \\ \hat{F}_I + \hat{I}_{Cl} &= \hat{F} \end{aligned} \quad (5)$$

The angular momentum operators \hat{I}_I and \hat{I}_{Cl} are associated with the nuclear spins of the iodine ($I_I = 5/2$) and chlorine ($I_{Cl} = 3/2$) atoms, respectively.

The complete set of $\text{CH}^{35}\text{ClFI}$ transitions was fitted and the spectroscopic parameters were obtained by a least-squares procedure.¹⁸ They are listed in Table 1 and reproduce the observed transitions with a standard deviation of 44 kHz. The unblended lines of the 5–20 GHz region are reproduced with a standard deviation of 2.3 kHz, within the experimental accuracy. As no lines for the $\text{CHF}^{37}\text{ClI}$ isotopologue were recorded in higher frequency, all the values of the centrifugal distortion parameters were fixed to the corresponding $\text{CHF}^{35}\text{ClI}$ values. The molecular parameters presented in Table 1 reproduced the 140 fitted lines with a standard deviation of 2.1 kHz.

All the observed and calculated frequencies for the two chlorine isotopomers $\text{CHF}^{35}\text{ClI}$ and $\text{CHF}^{37}\text{ClI}$ are given in upon request from the authors.

Ab initio calculations. The objective of the *ab initio* calculations is twofold: first, they are used to predict molecular parameters as accurately as possible in order to facilitate the assignment of the spectrum; secondly, a structure as close as possible to the equilibrium structure is calculated. All calculations were performed with GAUSSIAN 03²¹ and MOLPRO 2000.^{22,23}

The geometrical structure has been calculated at the second-order Møller–Plesset perturbation level of theory (MP2) using basis sets of different sizes. For the first row atoms (H, C, and F), the Dunning's correlation-consistent polarized valence triple zeta basis sets²⁴ were used. For chlorine which is a second row atom, these standard basis sets give rise to non-negligible errors. For this reason, the newly devised cc-

Table 1 Experimental values of rotational constants, centrifugal distortion constants, quadrupole coupling constants (iodine and chlorine nuclei) and spin-rotation constants (iodine nucleus) of CH³⁵CIFI and CH³⁷CIFI. Numbers in parentheses represent one standard deviation in units of the least significant digit. *Ab initio* values (when calculated) are given for CH³⁵CIFI

| Constant/MHz | CH ³⁵ CIFI | | CH ³⁷ CIFI |
|--|-----------------------|----------------------|-----------------------|
| | Experimental | <i>Ab initio</i> | Experimental |
| <i>A</i> | 6278.651148(129) | 6290.82 ^a | 6192.865335(197) |
| <i>B</i> | 1474.152806(76) | 1471.31 ^a | 1432.702503(173) |
| <i>C</i> | 1224.416397(104) | 1222.95 ^a | 1192.568955(193) |
| 10 ⁺⁴ <i>A_J</i> | 2.22294(52) | 2.15 ^b | 2.22294 ^c |
| 10 ⁺⁵ <i>A_{JK}</i> | -1.622(42) | -5.68 ^b | -1.622 ^c |
| 10 ⁺³ <i>A_K</i> | 7.25410(103) | 7.48 ^b | 7.25410 ^c |
| 10 ⁺⁵ <i>δ_J</i> | 4.66127(133) | 4.39 ^b | 4.66127 ^c |
| 10 ⁺⁴ <i>δ_K</i> | 9.3128(78) | 8.86 ^b | 9.3128 ^c |
| <i>χ_K</i> 10 ⁺⁸ | 1.847(116) | — | 1.847 ^c |
| Iodine nucleus | | | |
| <i>λ_{aa}</i> | -1704.58015(252) | | -1685.7418(42) |
| <i>λ_{bb}</i> | 838.57959 | | 820.3798 |
| <i>λ_{cc}</i> | 866.00056(244) | | 865.3620(47) |
| <i>λ_{ab}</i> | 699.7668(61) | | 731.8297(68) |
| <i>λ_{ac}</i> | 622.6878(160) | | 622.004(132) |
| <i>λ_{bc}</i> | -140.4346(265) | | -148.7207(247) |
| 10 ⁺³ <i>C_{aa}</i> | 4.786(162) | | 4.895(220) |
| 10 ⁺³ <i>C_{bb}</i> | 5.647(152) | | 5.95(37) |
| 10 ⁺³ <i>C_{cc}</i> | 5.753(164) | | 5.575(253) |
| 10 ⁺³ <i>C_{ab}</i> | -2.17(34) | | -2.18(46) |
| Chlorine nucleus | | | |
| <i>λ_{aa}</i> | -13.3970(34) | | -11.5924(59) |
| <i>λ_{bb}</i> | -15.4498 | | -11.2132 |
| <i>λ_{cc}</i> | 28.8468(38) | | 22.8056(67) |
| <i>λ_{ab}</i> | -51.3943(117) | | -40.5472(139) |
| <i>λ_{ac}</i> | -22.7366(201) | | -18.0474(234) |
| <i>λ_{bc}</i> | -21.107(40) | | -16.343(46) |

^a MP2/SDB-VTZ. ^b B3LYP/a'-VTZ-pp. ^c Experimental values fixed from the corresponding values of CH³⁵CIFI.

pV(T+d)Z²⁵ was used. Finally, for iodine, the correlation consistent polarized valence basis set with the Stuttgart–Dresden–Bonn (SDB) relativistic effective core potential,²⁶ SDB-cc-pVTZ^{27,28} was used. The calculated structural parameters are collected in Table 2 together with those calculated at the CCSD(T)/cc-pVDZ level of theory by Schwerdtfeger *et al.*⁷

Much effort was put into the calculation of the quartic centrifugal distortion constants in order to facilitate the prediction and the assignment of the high *J* and *K_a* transitions. The harmonic force field is required to calculate the quartic centrifugal distortion constants. Density functional theory was used with the Becke²⁹ three-parameter hybrid exchange functional and the Lee–Yang–Parr correlation functional (B3LYP).³⁰ This method is known to be inexpensive and remarkably accurate from the prediction of harmonic force fields.³¹ For this calculation, diffuse functions were used for fluorine (aug-cc-p-VTZ)³² and the small-core relativistic PP correlation consistent basis set (cc-pVTZ-PP)³³ was used for iodine. The calculated centrifugal distortion constants obtained using the B3LYP harmonic force field are given in Table 1.

The permanent electric dipole moment has been also calculated for CHFClI at the MP2/SDB-VTZ level of theory. The test of this level of theory has been performed on CH₃I, a similar molecule. The calculated value (1.62 D) is in good

Table 2 Structural parameters of CH³⁵CIFI, corresponding rotational constants and electric dipole moment obtained by *ab initio* calculations

| | CCSD(T) ^a cc-pVDZ | MP2 SDB-VTZ |
|-----------------------------|---------------------------------|----------------|
| <i>r_{C-I}</i> /pm | 218.9 | 214.69 |
| <i>r_{C-H}</i> /pm | 110.1 | 108.32 |
| <i>r_{C-F}</i> /pm | 135.9 | 134.96 |
| <i>r_{C-Cl}</i> /pm | 177.9 | 175.40 |
| ∠ HClI/° | 107.1 | 107.09 |
| ∠ ICF/° | 109.3 | 109.45 |
| ∠ ICCI/° | 113.3 | 112.23 |
| ∠ HCF/° | 109.6 | 109.65 |
| ∠ HCCI/° | 108.1 | 108.63 |
| ∠ FCCI/° | 109.4 | 109.73 |
| <i>A</i> /MHz | 6222.99 | 6290.82 |
| <i>B</i> /MHz | 1405.27 | 1471.31 |
| <i>C</i> /MHz | 1174.96 | 1222.95 |
| <i>μ</i> /D | | 1.33 |
| <i>μ_a</i> /D | | 0.23 |
| <i>μ_b</i> /D | | 0.21 |
| <i>μ_c</i> /D | | 1.30 |

^a Ref. 7.

agreement with the experimental value (1.64 D).³⁴ For CHFClI, we predicted that the three *a*-, *b*-, and *c*-type transitions should be observed in the pure rotational spectrum, with $\mu_a \approx \mu_b < \mu_c$ (see Table 2).

A complete set of spectroscopic parameters has been determined for the ground vibrational state, including the rotational and the centrifugal distortion constants, all the elements of the quadrupole coupling tensor for the iodine and the chlorine nuclei and spin-rotation constants for the iodine nucleus.

Inspection of Table 1 shows that the MP2/SDB-VTZ rotational constants are very close to the experimental ground state constants. This indicates that the equilibrium structure is close to the ground vibrational state structure which was expected for such a heavy molecule. Since only two different isotopomers (CHF³⁵ClI and CHF³⁷ClI) were investigated the structural information directly available from the experimental data is limited. Nevertheless, the *r_s*[Cl] coordinates of CHF³⁵ClI can be compared to those determined by *ab initio* calculations. The Kraitchman equations¹⁶ gave |*a_{Cl}*| = 223.5 pm, |*b_{Cl}*| = 76.3 pm, |*c_{Cl}*| = 5.3 pm (where *x_{Cl}*, *x* = *a*, *b*, *c* are the Cartesian coordinates in the *a*, *b*, *c* principal axis system). These results are in good agreement with the *ab initio* equilibrium values calculated at a MP2/SDB-VTZ level of theory: *a_{Cl}* = -222.8 pm, *b_{Cl}* = -76.3 pm, *c_{Cl}* = -6.0 pm.

The centrifugal distortion constants show higher discrepancies, around 5%. The relative difference of 250% on the *A_{JK}* constant is due to accidental cancellation of same order terms ($\Delta_{JK} = 3/8(\tau_{bbbb} + \tau_{aaaa}) - 1/4(\tau_{aacc} + \tau_{bbcc} + \tau_{ccaa}) = -0.6452 \text{ kHz} + 0.5883 \text{ kHz} = -0.0568 \text{ kHz}$ for CH³⁵CIFI).

Two independent quantities completely characterize the quadrupolar coupling tensor in its principal axis system: the χ_{zz} component of the tensor which measures the quadrupolar coupling in the bond direction, and the asymmetry parameter, $\eta = (\chi_{xx} - \chi_{yy})/\chi_{zz}$, which measures the deviation of the field-gradient tensor from axial symmetry.³⁵ The principal elements

χ_{xx} , χ_{yy} and χ_{zz} of the quadrupole coupling tensors were calculated by diagonalizing the quadrupole coupling tensors expressed in the a , b , c principal axis system. The small value for η (0.01917 for the iodine atom and 0.04011 for the chlorine atom) indicates that the z principal axis of the coupling quadrupole tensor nearly coincides with the carbon–halogen bond (C–X, X = I, Cl). CHFClI behaves like most of the molecules with one or several carbon–halogen bonds: the deviation from an axial charge distribution around the halogen nucleus is very weak^{36,37} indicating nearly cylindrical symmetry of the C–Cl and C–I bonds.

Rovibrational spectroscopy

The precise determination of the ground-state rotational constants of chlorofluoroiodomethane was an essential step before starting the rovibrational spectroscopy of two transitions involving the strong C–F stretching vibration, firstly the fundamental (ν_4) and then the first overtone ($2\nu_4$). The fundamental transition, predicted at 1081.4 cm^{-1} , should be a good candidate to evidence a parity violation effect between the two enantiomers, with the support of experimental techniques developed in Chardonnet's laboratory, either of the type saturation-spectroscopy⁵ or in the near future from a two-photon Ramsey fringe experiment on a molecular beam.¹² In relation with this latter project, the possibility of obtaining an infrared absorption spectrum of CHFClI from a continuous seeded supersonic expansion gives confidence for validating the principle of a parity violation measurement with a molecular beam. Although the very low rotational temperatures achieved in the supersonic expansion strongly limit the spectral range of possible coincidences with the CO₂ laser, about ten could be obtained with the P and R-branch transitions of the 9 μm band of the CO₂ laser, particularly if one considers a tuning range up to $\pm 15\text{ GHz}$ for sub-Doppler spectroscopy with frequency fixed lasers. High resolution infrared spectra can be now carried out and analysed in order to select among all the rovibrational transitions the most favourable molecular resonance with a CO₂ laser line.

Experimental results from supersonic jet and cell (at room temperature) coupled to a high resolution Fourier transform infrared (FTIR) spectrometer are presented as well as preliminary routes for the rovibrational analysis of CHFClI.

Fig. 1 displays two FTIR spectra of the ν_4 band of CHFClI recorded at 0.008 cm^{-1} resolution in a room temperature static cell (a) and in a supersonic expansion (b), respectively. The stick spectrum in Fig. 1c just serves to indicate some possible coincidences with P($J_{K_a K_c}$) and R($J_{K_a K_c}$) lines of the 9.4 μm band of the CO₂ laser. At the present time the spectral analysis is not advanced enough to propose some assignments of the hyperfine structure which could enable the selection of the most favorable resonance.

Fig. 2a displays a cell spectrum recorded in the same experimental conditions as that in Fig. 1a, but at full resolution (0.002 cm^{-1}) with an expanded view of P($J_{K_a K_c}$) lines in the region $1056\text{--}1057\text{ cm}^{-1}$. A characteristic PQR structure with a fine structure in the P and R branches is clearly visible for all the FTIR spectra. A significant variation of the intensity of the lines in the ν_4 vibration–rotation band as a

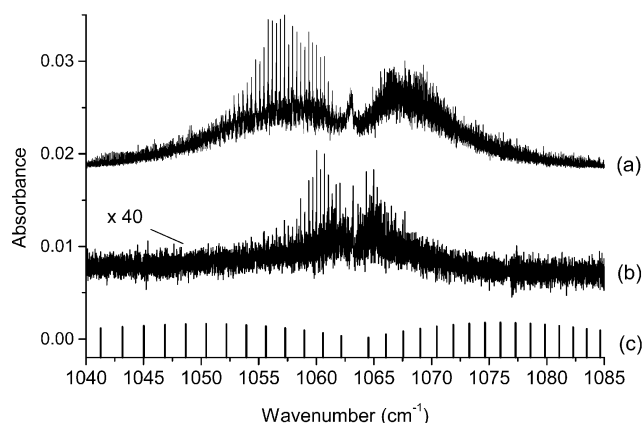


Fig. 1 FTIR spectra of the ν_4 band of CHFClI recorded at 0.008 cm^{-1} resolution (a) in a room temperature static cell; (b) in a supersonic expansion respectively; (c) stick spectrum of P($J_{K_a K_c}$) and R($J_{K_a K_c}$) lines of the 9.4 μm band of the CO₂ laser.

function of J is observed between cell and jet conditions. The separation $\Delta\nu_{\text{max}}^{\text{PR}}$ of the two maxima of the P and R branches being approximately proportional to $[(A + B + C)T]^{1/2}$ for an asymmetrical top molecule,³⁸ where A , B and C are the rotational constants in the ground state of the transition, one can estimate the rotational temperature of the jet spectrum to about 70 K, with a rotational distribution centered around $J_{\text{max}} = 10$.

Before starting the rovibrational analysis, several points must be examined in detail: firstly, the possible congestion of cell spectra resulting for a low symmetry molecule from several hot bands of the low frequency vibrations (five between 200 and 800 cm^{-1}), secondly the presence of two major isotopomers in natural abundance (CHF³⁵ClI = 75.8%, CHF³⁷ClI = 24.2%), thirdly the hyperfine structure of iodine which displays a large splitting in the microwave spectrum, and finally the occurrence of vibrational perturbations between ν_4 and other vibrational states near in energy.

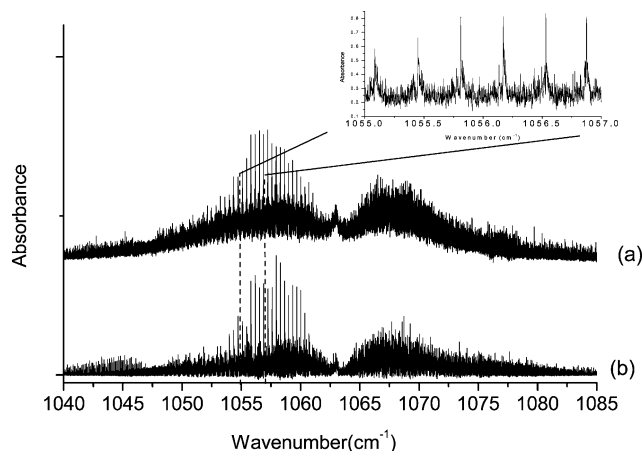


Fig. 2 (a) Cell spectrum recorded in the same experimental conditions as that in Fig. 1a, but at full resolution (0.002 cm^{-1}) with an expanded view of P($J_{K_a K_c}$) lines in the region $1056\text{--}1057\text{ cm}^{-1}$. (b) a first synthetic calculated spectrum about the ν_4 fundamental of CHFClI.

As a first result, only the isolated contribution of the ν_4 fundamental band, neglecting all types of interactions with other modes, is introduced and we proceed as follows. Taking advantage of the large spectral simplification due to jet cooling, a direct line-by-line assignment is made simpler for low J transitions, in order to determine approximate excited-state constants with fixing the ground state constants to the microwave results.³⁹ These spectroscopic parameters are then optimized using a least-squares fit with the program WANG⁴⁰ of about one thousand assigned lines and finally included in the 300 K cell spectrum at 0.002 cm^{-1} for refining the set of rotational constants, centrifugal distortion constants and band centers for each isotopomer. A first synthetic spectrum about the ν_4 fundamental of CHFClI is presented in Fig. 2b.

Synthesis of (+)- and (-)-CHFClI

For an accurate PV test it is necessary to have the two enantiomers of CHFClI available. Their synthesis was investigated by first resolving FClI CCO_2H and then by using a highly enantioselective decarboxylation reaction. For the resolution of chiral carboxylic acids, it is often convenient to use classical commercially available chiral amines to prepare diastereomeric salts and to resolve them by crystallization in an appropriate solvent.⁴¹ This method is convenient in our context because it will enable preparation of large quantities of enantiomerically enriched material for the subsequent spectroscopy in a supersonic beam, which requires large quantities of compound. Among the classical chiral amines tried for the resolution by crystallization, the best results were obtained with (-)-strychnine and either CHCl_3 or MeOH as solvent for the crystallization. Indeed, after one crystallization in CHCl_3 at room temperature of the 50:50 mixture $\{(\pm)\text{-FClI}\text{CCO}_2\text{H},(-)\text{-strychnine}\}$, the diastereomeric *n* salt **8a** *i.e.* $\{(+)\text{-FClI}\text{CCO}_2\text{H},(-)\text{-strychnine}\}$ crystallized with 67–72% diastereomeric excess (de). The diastereomeric excess could directly be read from the ^{19}F NMR spectrum of the salts in CDCl_3 at 200 MHz.⁴² An enantioenriched sample of (+)-CHFClI with 63.3% ee could subsequently be obtained by decarboxylation of the strychninium *n* salt with 67% de in triethyleneglycol at 110 °C and 100 mm Hg with 30% yield (Scheme 2).¹⁴ On the other hand, the use of MeOH enabled

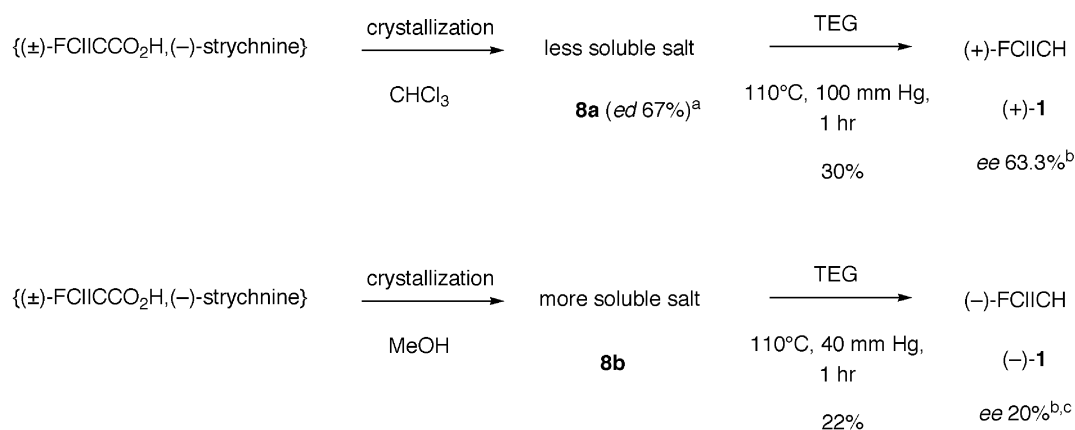
recovery from the mother liquors of the *p* salt **8b** *i.e.* $\{(-)\text{-FClI}\text{CCO}_2\text{H},(-)\text{-strychnine}\}$ less than 50% de. The decarboxylation of the strychninium *p* salt **8b** in triethyleneglycol at 110 °C and 40 mm Hg gave (-)-CHFClI with 20.5% ee and with 22% yield. Due to the high solubility of the strychninium *p* salt in MeOH, the (-) enantiomer was contaminated with MeOH.

The ee's of (+)- and (-)-CHFClI were determined by two different methods. For the (+) enantiomer, an ee of 63.3% was determined in Schurig's laboratory by analytical gas chromatography on a Chirasil- γ -Dex column under cryogenic conditions.^{43,44} The ee of the (-) enantiomer was measured *via* the host-guest complexation process of CHFClI by a chiral thiomethylated cryptophane ((-)-**7**) as described below.

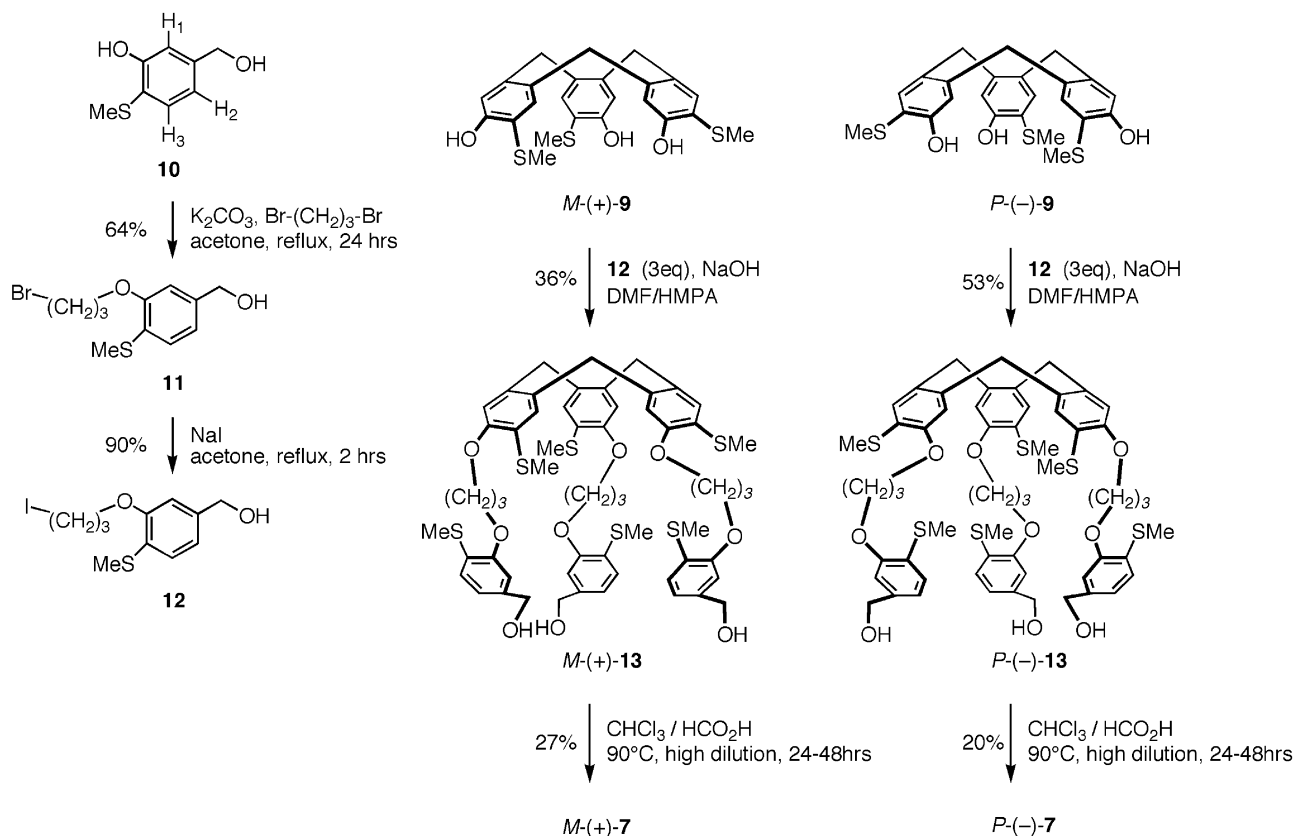
Enantioselective recognition of CHFClI by a chiral thiomethylated cryptophane

Cryptophane **7**⁴⁵ was prepared for the first time in enantiomerically enriched form, by using the template method which consists of cyclotrimerizing a resolved and functionalized cyclotrimeratrylene (CTV). Indeed, as described in Scheme 3, CTV's *M*-(+)- and *P*-(-)-**9** were prepared by an already known procedure⁵⁷ then functionalized to (+)- and (-)-**13** with appropriate benzylic alcohols **12** then cyclotrimerized under high dilution conditions. From a synthetic point of view, the templated method was found to be more efficient than the direct method described in ref. 45. However, because high temperature conditions were needed (up to 90 °C over 24–48 h), racemization occurred during this step. This is the reason why (+)- and (-)-**7** were obtained with 81.6 and 65.6% ee's (Fig. 3). The former ee's could be determined by analytical HPLC on a Regis (*S,S*) Whelk-O1 column (eluent hexane/THF 40 : 60).⁴⁶ This method is much more convenient than the former one using a less stable column (Chiralpak-OT(+)).⁴⁷ The two CD spectra of (+)- and (-)-**7** were also recorded and showed the same CD patterns as their CTV parents and allowed assignment of the *M*-(+) and *P*-(-) absolute configuration for **7**.

The molecular recognition process was observed by proton and fluorine NMR and appeared to be slow at these NMR timescales (as in the case of the chloroform complexation⁴⁵). Interestingly, cryptophane (\pm)-**7** forms with (+)- and (-)-**1**



Scheme 2 Synthesis of (+)- and (-)-**1** by decarboxylation of partially resolved strychninium salts **8a** and **8b**. ^a Diastereomeric excess determined by ^{19}F NMR in CDCl_3 , see ref. 14. ^b Enantiomeric excess determined by GC on a chiral stationary phase, see ref. 14. ^c Enantiomeric excess determined by ^{19}F NMR using cryptophane(-)-**7**.



Scheme 3 Synthesis of *M*-(+)- and *P*-(-)-cryptophane-E-(SCH₃)₆ **7** by the template method starting from resolved cyclotrimeratriylenes *M*-(+)- and *P*-(-)-**9**.

diastereomeric complexes which could be visualized by ¹H and ¹⁹F NMR in C₂D₂Cl₄ at 300 K (Fig. 4). Under these conditions, the respective association constants were found to be 37 M⁻¹ for the {*R*-(-)-**1** @ *P*-(-)-**7**} / {*S*-(+)-**1** @ *M*-(+)-**7**} diastereomer and 29 M⁻¹ for the {*S*-(+)-**1** @ *P*-(-)-**7**} / {*R*-(-)-**1** @ *M*-(+)-**7**} one (within 15% error) which revealed a low enantioselectivity. Cryptophane (-)-**7** was subsequently used to determine the ee of enantioenriched (-)-CHFClI. Indeed, the latter was found to be 23 ± 3% with the use of (-)-**7** having 65.6% ee by ¹⁹F NMR in C₂D₂Cl₄ at 300 K and at 471.4 MHz (see Fig. 5). More accurately a 20.5% ee was obtained for the same (-)-**1** sample when using analytical GPC on a Chirasil-γ-Dex column under cryogenic conditions.

Vibrational circular dichroism

Vibrational circular dichroism (VCD) which measures the difference in absorbance for left and right circularly polarized light for a vibrational transition, is a well established technique for identification of absolute configuration.^{48–50} The method involves comparison of observed VCD spectra with calculated VCD intensities for a specified enantiomer, carried out at the density functional theory (DFT) level.^{49,51}

Observed IR and VCD spectra are displayed in Fig. 6. Larger VCD noise was observed for the 1060 cm⁻¹ band because the maximum absorbance is near 1.4. Difficulties with racemization of the sample during the 6 h measurement and subsequent storage in the cell or on the vacuum line at room temperature with some exposure to fluorescent lights pre-

cluded additional measurements at reduced pressure and/or longer collection times.

The observed spectra show different band contours in the IR and VCD spectra for the same vibrational mode. In order to identify an absolute configuration, the measurements were made on a gas phase sample. Consequently, the VCD intensity must be integrated over the full rotational band contour of the spectrum for comparison with calculations about a non-rotating molecule. Such integration yields net positive VCD intensity for the band near 1060 cm⁻¹ (C–F stretch with C–H–Cl–I umbrella motion) and net negative VCD intensity for the band near 1170 cm⁻¹ (H–C–I deformation). The VCD intensity for the band at 1299 cm⁻¹ is too weak for accurate intensity measurement. The band contours will be discussed further below.

The five DFT calculations with a variety of functionals and basis sets yielded similar calculated frequencies and IR intensities, and the same VCD signs for all modes. The calculated frequencies, normal mode assignments and IR and VCD intensities are gathered in Table 3 for the B3LYP/SDD calculation, with comparison to observed frequencies obtained from Raman spectra of liquid CHFClI. This basis set gave the best agreement with observed relative IR and VCD intensities.

The observed IR and VCD spectra of the gas-phase sample are compared to the B3LYP/SDD calculation in Fig. 7. The anisotropy ratios ($g = \Delta A/A$) measured from peak areas of the observed IR and VCD bands centered at 1170 and 1060 cm⁻¹ are 2×10^{-5} and $+5 \times 10^{-5}$, respectively, approximately ten times larger than the corresponding calculated anisotropy

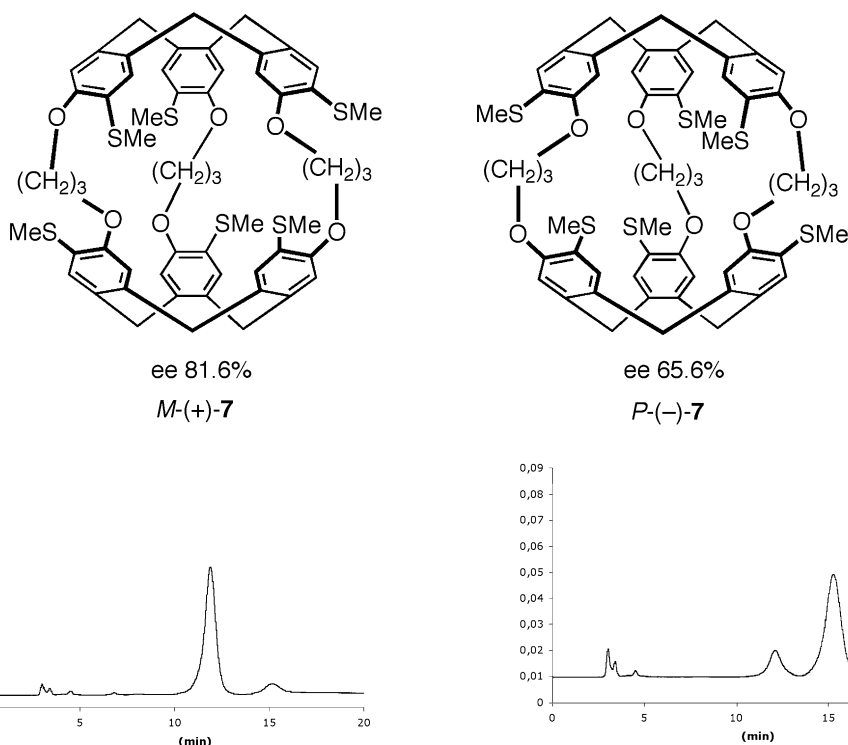


Fig. 3 Enantiomeric excess determination of *M*-(+)- and *P*-(-)-7 by HPLC on a Regis (*S,S*) Welk-O1 column (eluent THF/pentane 60 : 40, 1 ml min⁻¹).

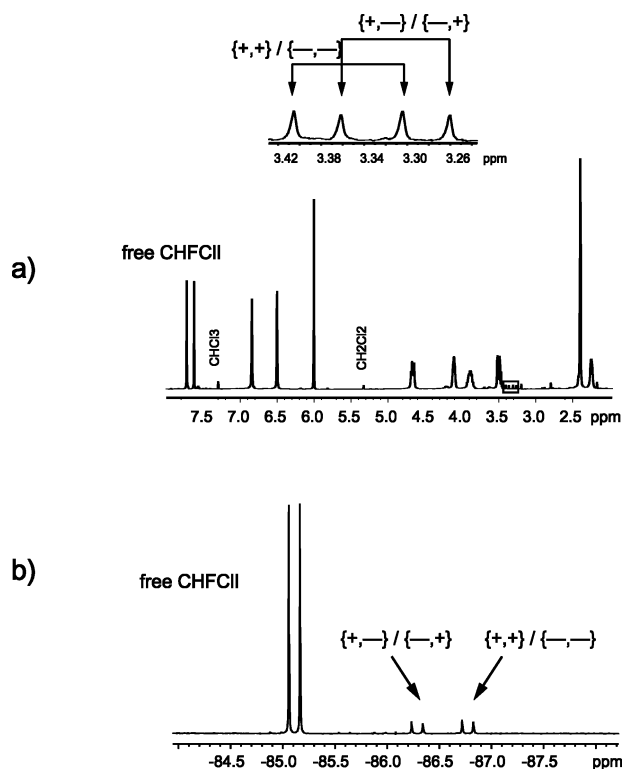


Fig. 4 Complexation process of of (\pm)-CHFCII 1 by (\pm)-cryptophane-E-(SCH₃)₆ 7 in C₂D₂Cl₄ and at 300 K. (a) ¹H NMR spectra at 500 MHz; the signals corresponding to the two diastereomeric complexes are expanded. b) ¹⁹F NMR spectra at 471.4 MHz.

ratios ($g = 4R/D$, from Table 3), 3×10^{-6} (1197 cm⁻¹) and $+6 \times 10^{-6}$ (990 cm⁻¹). We note, however, that the uncertainty in the measured anisotropy ratios is large, because of the VCD noise level.

From the agreement in sign of the integrated VCD intensity for the two prominent VCD features, the C–F stretch (1060 cm⁻¹, positive) and the H–C–I deformation (1170 cm⁻¹, negative) bands, and the corresponding bands in all five calculations, this study unambiguously identifies the absolute configuration as (*S*)-(+)-fluoroiodomethane, in agreement with the previous assignment based on DFT calculations of the specific rotation.¹⁴

Few studies of rotational-vibrational VCD have appeared in the literature.^{52–56} For our measurements of *trans*-dideuteriocyclopropane^{52,53,55} and *trans*-dideuteriooxirane,⁵⁴ with C₂ symmetry, the band contours for the IR and VCD were similar, and the sign of the P, Q and R rotational branches is the same for each mode. For gas-phase methyloxirane, Polavarapu⁵⁶ identified two modes for which the central Q-branch envelope had a sign opposite to that of the P- and R-branch envelopes. This observation was explained in terms of an accidental symmetric top molecule for which different components of the rotational strength scalar product contribute to different rotational branches. The rotational strength expression for mode *a* is

$$R^a = \text{Im}(\hat{\mu}_{01} \cdot \hat{m})_{10}$$

$$= \frac{\hbar}{2} \left[\left(\frac{\partial \mu_x}{\partial Q_a} \right)_0 \left(\frac{\partial m_x}{\partial P_a} \right)_0 + \left(\frac{\partial \mu_y}{\partial Q_a} \right)_0 \left(\frac{\partial m_y}{\partial P_a} \right)_0 + \left(\frac{\partial \mu_z}{\partial Q_a} \right)_0 \left(\frac{\partial m_z}{\partial P_a} \right)_0 \right] \quad (6)$$

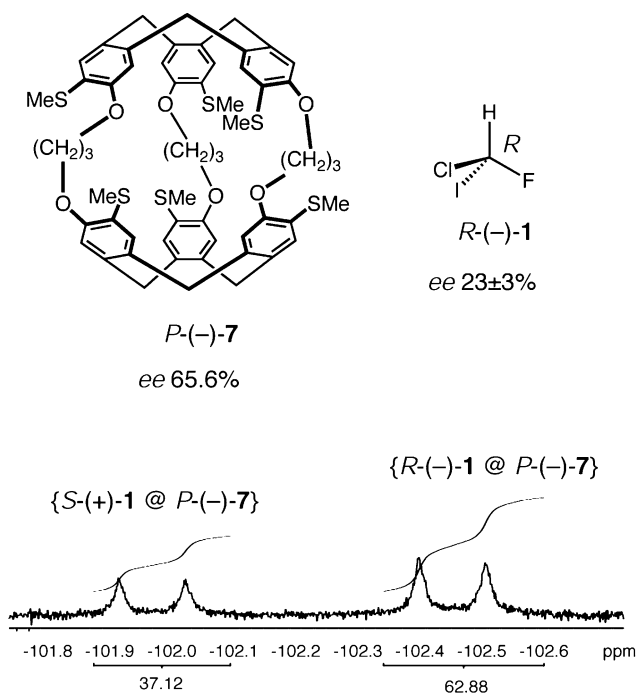


Fig. 5 Enantiomeric excess determination of (–)-1 by ^{19}F NMR in $\text{C}_2\text{D}_2\text{Cl}_4$ at 300 K using cryptophane (–)-7 as a chiral complexing agent. Two doublets corresponding to diastereomeric host–guest complexes $\{(+) \text{-}1 @ (-) \text{-}7\}$ and $\{(-) \text{-}1 @ (-) \text{-}7\}$.

where the scalar product of the dipole transition moments has been expressed in the last equality for components along axes x , y and z in the harmonic approximation, where Q_a is the normal mode, P_a is the conjugate momentum, μ is the electric dipole moment of the molecule and m is the magnetic dipole moment of the molecule. For the case of methyloxirane,⁵⁶ the $\Delta K = 0$, Q -branch transitions depend on the x -term in eqn (6) with the x -axis along the principal axis with least moment of inertia, whereas the $\Delta K = \pm 1$ branches depend on the y and z terms, along the intermediate (y) and largest moment of inertia axes (z). Since these individual components of the scalar product sum can have different signs, the rotational VCD band contour need not be monosignate nor identical to the absorption band contour. Chlorofluoroiodomethane is an asymmetric top with calculated moments of inertia ($\text{amu}\cdot\text{\AA}^2$) 86.8, 371.5 and 447.1 (0.195, 0.046, 0.038 cm^{-1}). As shown in Fig. 8, the B3LYP/SDD calculations place the dipole deriva-

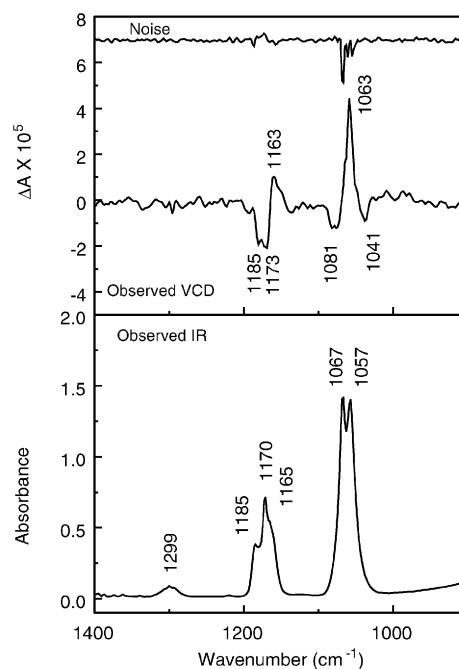


Fig. 6 IR (lower frame) and VCD (upper frame) spectra of (+)-fluoroiodochloromethane, ~ 100 torr, in 5 cm^{-1} gas cell equipped with BaF_2 windows, 4 cm^{-1} resolution, 6 h collection, instrument optimized at 1400 cm^{-1} .

tive for the C–F stretch (calculated frequency 989 cm^{-1}) in the yz -plane, with expected rotational band contour classified as a mixture of types B (with two prominent wings and a central minimum) and C (central peak and moderate wings). The dipole derivative for the H–C–I deformation (calculated frequency 1197 cm^{-1}) is in the xy -plane, with an expected hybrid band contour of type A (central maximum with weak wings) and B. It is interesting to note that the experimental IR band contour for the C–F stretch appears to be dominated by the type B contribution with two prominent wings and a central minimum, whereas the VCD contour for this band exhibits a central peak and moderate wings (of the opposite sign) characteristic of the type C contribution. The VCD band contour exhibits a central branch of same sign as the high-frequency wing and of opposite sign with respect to the low-frequency wing. Further analysis of the band contours is not possible without higher quality VCD spectra.

Table 3 Observed and calculated normal modes of CHClFI

| Mode | Observed frequency (Raman) | Calculated frequency (DFT B3LYP/sdd; unscaled) | $10^{40} \times$ Calculated dipole strength/ $\text{esu}^2\text{ cm}^2$ | $10^{44} \times$ Calculated rotational strength/ $\text{esu}^2\text{ cm}^2$ | Assignment (largest contribution) |
|------|----------------------------|--|---|---|-----------------------------------|
| 1 | 197 | 185 | 0.4 | 0.1 | Cl–Cl–I deformation |
| 2 | 274 | 259 | 1.8 | –0.3 | F–C–I deformation |
| 3 | 418 | 371 | 14.2 | 0.5 | Cl–C–F deformation |
| 4 | 587 | 563 | 356.5 | –12.7 | C–I stretch |
| 5 | 764 | 684 | 1237.3 | 10.1 | C–Cl stretch |
| 6 | 1053 | 990 | 837.7 | 6.7 | C–F stretch |
| 7 | 1180 | 1197 | 284.2 | –4.5 | H–C–I deformation |
| 8 | 1301 | 1286 | 49.3 | 0.6 | H–C–F deformation |
| 9 | 3150 | 3215 | 5.6 | –1.7 | C–H stretch |

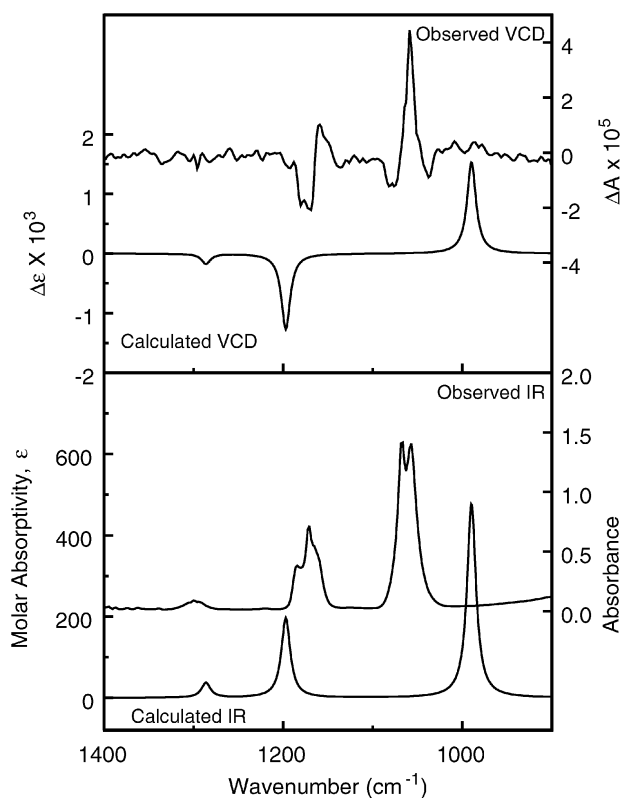


Fig. 7 Comparison of IR (lower frame) and VCD (upper frame) observed for (+)-CHFClI in the gas phase (right axes) and calculated for (S)-CHFClI (left axes) at the DFT level, B3LYP functional, SDD basis set (6 cm^{-1} half-width Lorentzian bands).

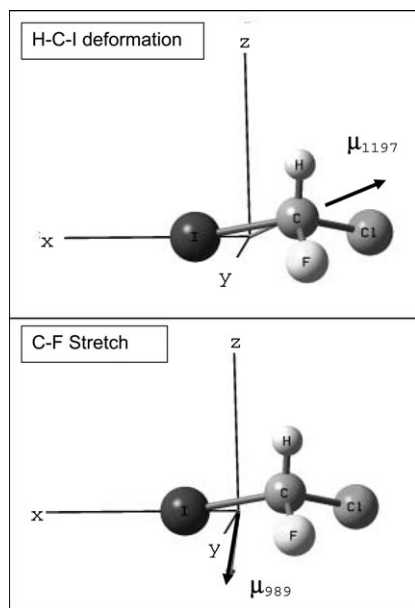


Fig. 8 Calculated geometry, inertial axes and dipole derivatives (μ , with subscript indicating calculated frequency in cm^{-1}) for (S)-CHFClI, (DFT: (B3LYP functional/SDD basis set), for two normal modes.

Conclusion

A complete investigation has been conducted on chlorofluoroiodomethane, one of the most simple model chiral molecule. Racemic CHFClI has been synthesized in multigram quantities, its spectroscopic parameters for the vibrational ground state have been determined by microwave spectroscopy whereas the rovibrational analysis of the C–F stretching band is under investigation. This spectroscopic analysis is one of the most important steps in the perspective of future ΔE_{PV} measurements by ultrastable CO_2 laser spectroscopy because it will enable selection of the most appropriate absorption line for the final PV test. For this purpose it has been shown that it is possible to prepare the two partially enriched *S*-(+) and *R*-(–)-1 enantiomers, whose absolute configuration has been determined by VCD studies in the gas phase. Finally, the enantioselective complexation process by a chiral cryptophane has shown to be effective and to be a practical tool for ee measurements. For future work, a way to improve the enantiomeric enrichment of (+)- and (–)-CHFClI would be to use gas chromatography on a chiral phase on the preparative scale.

Experimental

1. Sample preparation

General. ^1H -, ^{13}C - and ^{19}F -NMR spectra were recorded on a Bruker DPX 200 spectrometer (at 200 MHz for ^1H , 50.4 MHz for ^{13}C and 188.6 MHz for ^{19}F) and on a Varian Unity + spectrometer (at 500 MHz for ^1H and 471.4 MHz for ^{19}F). Melting or decomposition temperatures were measured using a Perkin-Elmer DSC7 microcalorimeter. Elemental analyses were carried out by the Service Central d'Analyses, CNRS. Specific rotations (in $^\circ\text{ cm}^2\text{ g}^{-1}$) were measured in a 1 dm thermostated quartz cell on a Jasco-P1010 polarimeter. Circular dichroism spectra were recorded on a CD6 Jobin-Yvon dichrograph. $[\text{D}_2]$ tetrachloroethane was purchased from Eurisotop. Compounds **2**, **4**, **5**, **6** and (+)-**1** were prepared as previously described.¹⁴ Cyclotrimeratrylenes (+)- and (–)-**9** and benzylic alcohol **10** were prepared according to literature.⁵⁷

(±)-Chlorofluoroiodomethane ((±)-1). 25 g (43.6 mmol) of the {(±)-**2**, (–)-strychnine} salt in triethyleneglycol TEG (100 mL) was decarboxylated, by heating at $110\text{ }^\circ\text{C}$, under 110 mmHg, and under stirring for 1 h. 2.8 g (33%) of (±)-**1** was collected in a liquid nitrogen trap. ^1H NMR (CDCl_3) δ 7.62 (d, $^2J_{\text{HF}} = 50.2$ Hz). ^{13}C NMR (CDCl_3) δ 55.04 (d, $^1J_{\text{CF}} = 308.4$ Hz). ^{19}F NMR (CDCl_3 ; CFCl_3 as internal reference) δ –86.99 (d, $^2J_{\text{HF}} = 50.2$ Hz). ^{19}F NMR (CDCl_3 ; $\text{CF}_3\text{CO}_2\text{H}$ as internal reference) δ –11.03 (d, $^2J_{\text{HF}} = 50.3$ Hz) in agreement with literature data.¹¹

(–)-Chlorofluoroiodomethane ((–)-1). A solution of 6.57 g of the {(±)-**2**, (–)-strychnine} salt in 35 mL of MeOH was allowed to crystallize at room temperature for one day under stirring. After filtration, 3.758 g (57%) of the {(+)-FCI CCO_2H ,(–)-strychnine} salt **8a** was obtained as a yellow precipitate, de 67% (determined by ^{19}F NMR in CDCl_3 at

200 MHz). From the mother liquors, after evaporation of the solvent, 2.644 g (40%) of the $\{(-)\text{-FCIICCO}_2\text{H}, (-)\text{-strychnine}\}$ salt **8b** was obtained, and subsequently decarboxylated in TEG (10 mL) by heating at 110 °C, under 40 mmHg, and under stirring for 1 h. 200 mg (22%) of $(-)\text{-1}$ was collected in a liquid nitrogen trap. Enantiomeric excess 20.5% (analytical gas chromatography on a Chirasil- γ -Dex column under cryogenic conditions¹⁴).

3-[(3-bromopropyl)oxy]-4-methylthiobenzenemethanol 11. A mixture of 3-hydroxy-4-methylthiobenzyl alcohol (4.64 g, 27 mmol), K_2CO_3 (3.88 g, 28 mmol) and 1,3-dibromopropane (6 mL, 58 mmol) in acetone (50 mL) was refluxed for 24 h. The solvent was stripped off and the residue was taken up in a mixture of water and diethyl ether. The organic layer of the filtrate was washed with aqueous (10%) KOH, with water, dried over sodium sulfate and evaporated. Column chromatography ($\text{CH}_2\text{Cl}_2/\text{AcOEt}$ 9 : 1) gave 5.08 g (64%) of pure 3-[(3-bromopropyl)oxy]-4-methylthiobenzenemethanol **11**. Mp 83 °C. $^1\text{H NMR}$ (CDCl_3) 7.09 (d, H_3 , $^3J_{32} = 8.0$ Hz); 6.88–6.94 (m, H_1 and H_2); 4.63 (d, CH_2OH , $^3J = 5.0$ Hz); 4.17 (t, OCH_2 ; $^3J = 5.5$ Hz); 3.66 (t, CH_2Br , $^3J = 6.5$ Hz); 2.40 (s, SCH_3); 2.35 (qi, CH_2 , $^3J = 6.0$ Hz); 1.64 (t, CH_2OH , $^3J = 5.0$ Hz). $^{13}\text{C NMR}$ (CDCl_3) 155.3 (ArC–O); 138.8 (ArC–C); 126.8 (ArC–S); 125.7 (ArC₃); 119.9 (ArC₂); 110.1 (ArC₁); 66.0 (CH_2O); 64.9 (CH_2OH); 32.3 (CH_2); 30.1 (CH_2Br); 14.5 (SCH_3). Anal calc for $\text{C}_{11}\text{H}_{15}\text{O}_2\text{SBr}$: C, 45.37; H, 5.19. Found: C, 45.3; H, 5.2.

3-[(3-iodopropyl)oxy]-4-methylthiobenzenemethanol 12. A mixture of 3-[(3-bromopropyl)oxy]-4-methylthiobenzenemethanol **11** (2.71 g, 9.3 mmol) and NaI (3.19 g, 21.3 mmol) in acetone (25 mL) was refluxed at 40 °C for 2 h. The solvent was evaporated and the residue was taken up in a mixture of water and dichloromethane. The aqueous layer was extracted with dichloromethane, the organic layer was dried over sodium sulfate and evaporated to dryness to give pure **12** (2.84 g, 90). Mp 79 °C. $^1\text{H NMR}$ (CDCl_3) 7.09 (d, H_3 , $^3J_{32} = 8.0$ Hz); 6.88–6.94 (m, H_1 and H_2); 4.63 (d, CH_2OH , $^3J = 6.0$ Hz); 4.10 (t, OCH_2 , $^3J = 5.5$ Hz); 3.42 (t, CH_2I , $^3J = 6.5$ Hz); 2.40 (s, SCH_3); 2.30 (qi, CH_2 , $^3J = 6.0$ Hz); 1.68 (t, CH_2OH , $^3J = 6.0$ Hz). $^{13}\text{C NMR}$ (CDCl_3) 155.2 (ArC–O); 138.8 (ArC–C); 126.8 (ArC–S); 125.7 (ArC₃); 119.2 (ArC₂); 110.1 (ArC₁); 67.9 (OCH_2); 64.9 (CH_2OH); 32.9 (CH_2); 14.5 (SCH_3); 2.8 (CH_2I). Anal calc for $\text{C}_{11}\text{H}_{15}\text{O}_2\text{SI}$: C, 39.07; H, 4.47. Found: C, 39.3; H, 4.5.

***M*-(+)- and *P*-(-)-2,7,13-tris[3-[5-(hydroxymethyl)-2-thiomethylphenoxy]-propyloxy]-3,8,13-trithiomethyl-10,15-dihydro-5H-tribenzo[a,d,g]cyclononene *M*-(+)- and *P*-(-)-13.** To a solution of cyclotrimeratrilene *M*-(+)-**9** (80 mg, 176 μmol) in 4.8 mL of DMF/HMPA (1 : 1) was added 100 μl of aqueous NaOH (6.25 M) and the mixture was stirred under argon for 10 min, followed by addition of iodide **10** (0.18 g, 526 μmol). After the mixture was stirred at rt for 1 h, further amounts of NaOH (100 μl) and **10** (0.18 g) were added. After a night, the reaction mixture was poured into water and extracted with ethyl acetate. The organic layer was washed with aqueous HCl (1 M), with water, dried over sodium sulfate and evaporated to dryness. Column chromatography (dichloromethane/acetone

8 : 2) gave *M*-(+)-**13** (70 mg, 36%). $[\alpha]_{\text{D}}^{25} + 122$ (c 0.08, dioxane). Mp 300 °C (decomp). $^1\text{H NMR}$ (CDCl_3) 6.82–7.10 (m, aromatic H); 4.69 (d, H_a , $^2J = 13.5$ Hz); 4.53 (d, CH_2OH , $^3J = 5.5$ Hz); 4.22 (m, OCH_2); 3.56 (d, H_e , $^2J = 13.5$ Hz); 2.25–2.35 (2s, SCH_3 and m, CH_2); 1.71 (t, CH_2OH , $^3J = 5.5$ Hz). $^{13}\text{C NMR}$ (CDCl_3) 155.4 and 154.5 (ArC–O); 138.8, 137.6 and 132.0 (ArC–C); 128.3 (ArC–H); 126.6 (ArC–S); 125.5 (ArC–H); 125.2 (ArC–S); 119.7, 112.8 and 110.0 (ArC–H); 77.2 (CH_2OH); 65.1 and 65.0 (OCH_2); 36.3 (Ar– CH_2 –Ar); 29.2 (O– CH_2 – CH_2 – CH_2 –O); 14.5 and 15.1 (SCH_3). Anal calc for $\text{C}_{57}\text{H}_{66}\text{O}_9\text{S}_6$: C, 62.95; H, 6.12; S, 17.69. Found: C, 63.1; H, 6.2; S, 17.5.

The same procedure starting from 110 mg of *P*-(-)-**9** gave *P*-(-)-**13** (140 mg, 53%). -108 (c 0.32, dioxane).

Cryptophanes *M*-(+)- and *P*-(-)-7. To 160 mL of 99% formic acid stirred at 90 °C, was added dropwise a solution of triol *M*-(+)-**13** (70 mg, 64 μmol) in CHCl_3 (15 mL) for 24 h. Then the solution was stirred for 22 h at 90 °C. The solution became yellow and heterogenous. The solvent was evaporated under vacuum (some CHCl_3 was added at the end in the order to facilitate formic acid removal through azeotrope formation). Column chromatography (CH_2Cl_2) provided 17.7 mg (27%) of *M*-(+)-**7**.⁵⁸ Enantiomeric excess 81.6% (HPLC on a Regis (*S,S*) Welk-O1 column; eluent THF/pentane 60 : 40, 1 ml min^{-1} , wavelength 230 nm). CD ($1.07 \cdot 10^{-4}$ M in CH_2Cl_2) 245.2 (38.7), 273.2 (–38.2), 291.2 (–29.8), 306.6 (20.9), 312.4 (21.2). Mp 300 °C (decomp). $^1\text{H NMR}$ (CDCl_3) 6.84 (s, H_β); 6.49 (s, H_α); 4.63 (d, H_a , $^2J = 13.5$ Hz); 4.07 (m, O–CH– H'); 3.85 (m, O–CH'– H); 3.47 (d, H_e , $^2J = 13.5$ Hz); 2.37 (s, SCH_3); 2.22 (m, CH_2). $^{13}\text{C NMR}$ (CDCl_3) 153.8 (ArC–O); 135.9 and 131.3 (ArC–C); 125.4 (ArC–S); 125.2 and 110.9 (ArC–H); 63.8 (OCH_2); 36.4 (Ar– CH_2 –Ar); 30.2 (CH_2); 14.8 (SCH_3). Identical to literature.⁴⁵

The same procedure starting from 127 mg of *P*-(-)-**13** gave *P*-(-)-**7** ((24.1 mg, 20%). Enantiomeric excess 65.6% (HPLC on a Regis (*S,S*) Welk-O1 column; eluent THF/pentane 60 : 40, 1 ml min^{-1} , wavelength 230 nm). CD ($8.42 \cdot 10^{-5}$ M in CH_2Cl_2) 245.6 (–29.4), 274.8 (32.4), 293 (30), 309 (–15.6), 311.8 (–16.6).

NMR experiments. The sample consisting of (\pm)-cryptophane-E-(SCH_3)₆ and (\pm)-CHFCII was prepared by mixing 5 mg (4.8 μmol) of (\pm)-**7** and 1 μl (11.8 μmol) of (\pm)-**1** in 0.7 mL of $\text{C}_2\text{D}_2\text{Cl}_4$. The sample consisting of (–)-cryptophane-E-(SCH_3)₆ and (–)-CHFCII was prepared by mixing 3 mg (2.9 μmol) of (–)-**7** and 1.7 μl (20.4 μmol) of (\pm)-**1** in 0.7 mL of $\text{C}_2\text{D}_2\text{Cl}_4$. Each experiment was performed twice.

Fourier transform microwave spectrometer. Rotational spectra in the 6–20 GHz spectral range were recorded using the Lille FTMW spectrometer.⁵⁹ A gas mixture of 3 mbar of CHClFI completed with neon as carrier gas to a total pressure of 1 bar was prepared. Gas pulses were then expanded into the vacuum tank through a pulsed nozzle to create a supersonic beam. The supersonic beam cools the gas to a few Kelvin which considerably reduces the number of observable transitions. Gas pulses are introduced into the vacuum tank by means of a pulsed solenoid nozzle. The molecules are then polarized by a microwave pulse and the molecular free

induction decay signal, after amplification is frequency down-converted. As the nozzle is inserted in the centre of the fixed mirror of the Fabry-Perot cavity, the supersonic expansion is parallel to the optical axis of the cavity. Each transition is divided into two Doppler components. The central frequencies of the lines are determined by averaging the frequencies of the two Doppler components after transformation of 4096 data points time domain signal, leading to a digital resolution of 2.4 kHz in the spectrum. The accuracy of frequency measurements is estimated to be better than 3 kHz. The linewidth for a typical, well-resolved line is 10 kHz. Such a high resolution spectrum is shown in Fig. 9 (part of the $4_{13} \leftarrow 3_{03}$ transition around 17 GHz). The three μ_a , μ_b , μ_c -types of transition have been observed. At the same microwave pulse length, the optimal microwave powers to polarize the molecules were found to be around 20 mW for μ_a , μ_b type transitions and 4 mW for μ_c -type transitions, respectively (which indicates that $\mu_c > \mu_b \approx \mu_a$ in agreement with the *ab initio* predictions). All the FTMW data were weighted according to the frequency measurement accuracy (3 kHz).

Millimetre spectra. Several high- J lines of CHClFI have been observed at room temperature in the 270–350 GHz range and recorded at a pressure of about 0.13 mbar. All spectra were measured with the Lille computer-controlled MMW spectrometer using a phase-stabilized backward-wave-oscillator source and a He-cooled InSb bolometer (Queen Mary College) detector. The accuracy of the measurements is equal to 50 kHz. However several lines are broadened by the quadrupole hyperfine structure or the K degeneracy, and can only be resolved when the frequency difference reaches 400 kHz. All these blended lines were individually weighted, between two and four times the measurement accuracy, in accordance with the obs – calc values. This procedure was

carefully applied in order to not bias the fit, and for reaching as meaningful frequencies as possible.

Rovibrational spectroscopy. Our continuous supersonic jet-FTIR spectrometer device has been described in detail elsewhere.⁶⁰ Briefly, CHFClI is seeded in argon at about 40% by sweeping the rare gas over the chiral molecule maintained at room temperature in a pyrex flask. The CHFClI/Ar mixture is then expanded at a stagnation pressure of about 700 mbar through a circular nozzle of 250 μm diameter and evacuated by a 18 $\text{m}^3 \text{h}^{-1}$. Varian four stage diffusion pump backed by a 400 $\text{m}^3 \text{h}^{-1}$. Roots pump (Edwards EH 500) and a Leybold D60 (60 $\text{m}^3 \text{h}^{-1}$) rotary vane pump. In these conditions, the background pressure is typically equal to 10^{-3} mbar with a stagnation pressure of 700 mbar. The supersonic expansion is probed about 2 mm in front of the nozzle by the IR beam coming from a Bruker IFS 120 HR interferometer, which intersects the molecular beam 16 times, crosses a bandpass filter centred around 1060 cm^{-1} (FWHM = 300 cm^{-1}) and finally focusses on a HgCdTe photovoltaic detector (cut-off at 16 μm).

The small available quantity of racemic CHFClI synthesized (4.3 g) for these continuous gas flow experiments represents a strong limitation to obtain a complete set of excited-state rotational constants, centrifugal distortion constants and band centers with a sufficient accuracy. Therefore our experimental strategy is based on the following considerations: firstly, with a throughput of 1 mol h^{-1} and in our seeded jet conditions, the whole CHFClI is consumed after only 20 min of recording. From the LN₂ cooling traps installed at the end of the pumping system, about 85% of iodochlorofluoromethane injected was recovered after each cycle and could be reused without purification, which increased the recording time by a factor of four. Secondly, scan-by-scan acquisition mode of the

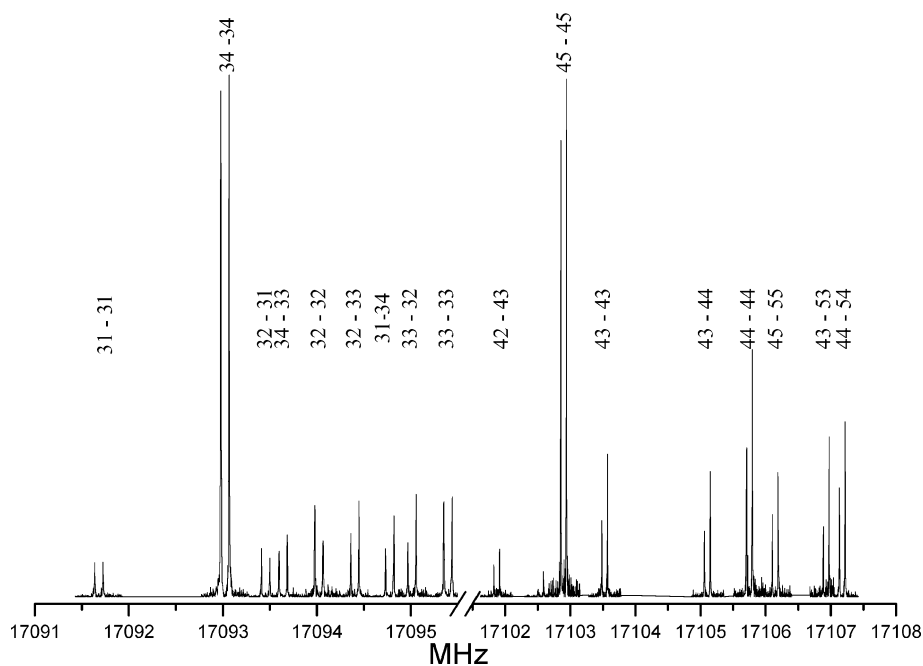


Fig. 9 Part of the well resolved $F_1 = 3 \leftarrow 3$ and $4 \leftarrow 4$ components of the $J_{K_a K_c} = 4_{13} \leftarrow 3_{03}$ transition of $\text{CHF}^{35}\text{ClI}$. The figure is obtained by concatenation of several high resolution spectra obtained after Fourier transformation of 100 coadded free induction decays.

interferograms was operated in order to record an individual phase correction, which contributes to significantly lower the statistical noise of the spectrum. In these conditions, the resulting jet spectrum is the Fourier transform of 50 coadded interferograms recorded at 0.008 cm^{-1} resolution.

The remaining quantity of CHFCII (about 1 g) was used for cell experiments. The vacuum chamber of our molecular beam device is used as a room temperature static cell with a volume of 50 dm^3 and an absorption length of 5 m, which enables injection of low sample pressures (0.05 mbar for the ν_4 band of CHFCII). The maximum optical path difference of our Bruker FTIR spectrometer is 2.25 m, resulting in an instrumental bandwidth (full width at half maximum) of 0.0022 cm^{-1} (unapodized) or 0.002 cm^{-1} (with boxcar apodization). Two cell spectra, which represent the Fourier transform of 150 and 75 coadded interferograms, have been recorded at 0.008 and 0.002 cm^{-1} resolution, respectively. During the static cell experiments, a significant evolution in the band contour of the C–F stretching band of CHFCII is observed after 40 min of recording. This is interpreted as resulting from the slow decomposition of the product, and consequently the vacuum chamber is evacuated and fresh CHFCII is reinjected after each cycle of ten scans.

Gas phase VCD spectroscopy. A sample of (+)-CHFCII (ee 50%) was transferred on a vacuum line into a 5 cm pathlength gas cell with BaF_2 windows by condensing into a side-arm of the cell. Spectra were obtained for the gas phase at ambient vapor pressure ($\sim 100\text{ torr}$). IR and VCD spectra were measured on a modified ChiralIR VCD spectrometer (BioTools, Inc., Wauconda, IL) equipped with dual PEM optics to minimize baseline artifacts.⁶¹ VCD spectra were recorded for 6 h in 1 h blocks, at 4 cm^{-1} resolution.

Calculations: Optimized geometries, vibrational frequencies and IR and VCD intensities were calculated at the DFT level with Gaussian 03²¹ with a variety of basis sets and functionals for the (*S*)-enantiomer (B3LYP functional with LanL2DZ,^{62–64} CEP-121G,⁶⁵ and SDD⁶⁶ basis sets; B3PW91 functional with LanL2DZ basis set). Calculated intensities were converted to Lorentzian bands with 6 cm^{-1} half-width for comparison to experiment.

Acknowledgements

Professor Schurig and Dr Jiang are warmly thanked for their help in measuring the ee's of CHFCII samples with their GPC apparatus. Professor Roussel and Dr Vanthuynne are also warmly thanked for their help in finding the wright conditions for the analytical HPLC separation of cryptophanes. Part of this work was supported by the Institut du Développement et des Ressources en Informatique Scientifique (IDRIS), contract 41715. Fabrice Willaert is thanked for the millimetre wave measurements.

References

- 1 T. D. Lee and C. N. Yang, *Phys. Rev.*, 1956, **104**, 254–258.
- 2 It has already been observed in nuclear and atomic physics. See (a) C. S. Wu, E. Ambler, R. W. Hayward, D. D. Hoppes and R. P. Hudson, *Phys. Rev.*, 1957, **105**, 1413–1415; (b) M. A. Bouchiat and C. C. Bouchiat, *Phys. Lett.*, 1974, **48B**, 111–114; (c) L. M. Barkov and M. S. Zolotarev, *JETP*, 1980, **52**, 360–376; (d) M. A. Bouchiat and C. C. Bouchiat, *Rep. Prog. Phys.*, 1997, **60**, 1351–1396; (e) C. S. Wood, S. C. Bennett, D. Cho, B. P. Masterson, J. L. Roberts, C. E. Tanner and C. E. Wieman, *Science*, 1997, **275**, 1759–1763.
- 3 M. Quack, *Angew. Chem., Int. Ed. Engl.*, 1989, **28**, 571–586.
- 4 E. Arimondo, P. Glorieux and T. Oka, *Opt. Commun.*, 1977, **23**, 369–372.
- 5 (a) C. Daussy, T. Marrel, A. Amy-Klein, C. T. Nguyen, C. J. Bordé and C. Chardonnet, *Phys. Rev. Lett.*, 1999, **83**, 1554–1557; (b) C. Chardonnet, C. Daussy, T. Marrel, A. Amy-Klein, C. T. Nguyen and C. J. Bordé in *Parity violation in atomic physics and electron scattering*, eds. B. Frois and M. A. Bouchiat, World Scientific, New-York, 1999, pp. 325–355; (c) C. Chardonnet, T. Marrel, M. Ziskind, C. Daussy, A. Amy-Klein and C. J. Bordé, *J. Phys. IV*, 2000, **10-Pr8**, 45–54; (d) M. Ziskind, T. Marrel, C. Daussy and C. Chardonnet, *Eur. Phys. J.*, 2002, **20**, 219–225.
- 6 (a) J. Crassous, C. Chardonnet, T. Saue and P. Schwerdtfeger, *Org. Biomol. Chem.*, 2005, **3**, 2218–2224; (b) J. Crassous, F. Monier, J.-P. Dutasta, M. Ziskind, C. Daussy, C. Grain and C. Chardonnet, *ChemPhysChem*, 2003, **4**, 541–548; (c) J. Crassous and A. Collet, *Enantiomer*, 2000, **5**, 429–438.
- 7 P. Schwerdtfeger, J. K. Laerdahl and C. Chardonnet, *Phys. Rev. A*, 2002, **65**, 042508.
- 8 See J. K. Laerdahl and P. Schwerdtfeger, *Phys. Rev. A*, 1999, **60**, 4439–4453 and references therein.
- 9 P. Schwerdtfeger and R. Bast, *J. Am. Chem. Soc.*, 2004, **126**, 1652.
- 10 R. N. Haszeldine, *J. Chem. Soc.*, 1952, 4259–4267.
- 11 (a) I. Novak, D. B. Li and A. W. Potts, *J. Phys. Chem. A*, 2002, **106**, 465–468; (b) D. B. Li, S.-C. Ng and I. Novak, *Tetrahedron*, 2002, **58**, 5923–5926.
- 12 A. Shelkovich, C. Grain, R. J. Butcher, A. Amy-Klein, A. Goncharov and C. Chardonnet, *IEEE J. Quantum Electron.*, 2004, **40**, 1023–1029.
- 13 (a) J. Canceill, L. Lacombe and A. Collet, *J. Am. Chem. Soc.*, 1985, **107**, 6993–6996; (b) J. Costante-Crassous, T. J. Marrone, J. M. Briggs, J. A. McCammon and A. Collet, *J. Am. Chem. Soc.*, 1997, **119**, 3818–3823; (c) J. Crassous and S. Hediger, *J. Phys. Chem. A*, 2003, **107**, 10233–10240.
- 14 J. Crassous, Z. Jiang, V. Schurig and P. Polavarapu, *Tetrahedron: Asymmetry*, 2004, **15**, 1995–2001.
- 15 H. W. Kroto, *Molecular Rotation Spectra*, Dover Publications, New York, 1975.
- 16 W. Gordy and R. L. Cook, *Microwave Molecular Spectra*, Wiley, New York, 1984.
- 17 P. Thaddeus, L. C. Krisher and J. H. N. Loubser, *J. Chem. Phys.*, 1964, **40**, 257.
- 18 H. M. Pickett, *J. Mol. Spectrosc.*, 1991, **148**, 371.
- 19 J. Bierón, V. Kellö, P. Pyykkö, A. J. Sadlej and D. Sundholm, *Phys. Rev. A*, 2001, **64**, 052507.
- 20 D. Sundholm and J. Olsen, *J. Chem. Phys.*, 1993, **98**, 7152.
- 21 J. A. Pople *et al.*, *GAUSSIAN 03 (Revision B.04)*, Gaussian Inc., Pittsburgh PA, 2003.
- 22 *MOLPRO 2000* is a package of *ab initio* programs written by H.-J. Werner *et al.*
- 23 P. J. Knowles, C. Hampel and H.-J. Werner, *J. Chem. Phys.*, 2000, **112**, 3106.
- 24 T. H. Dunning Jr., *J. Chem. Phys.*, 1989, **90**, 1007.
- 25 T. H. Dunning Jr., K. A. Peterson and A. K. Wilson, *J. Chem. Phys.*, 2001, **114**, 9244.
- 26 A. Bergner, M. Dolg, W. Küchle, H. Stoll and H. Preuss, *Mol. Phys.*, 1993, **80**, 1431.
- 27 J. M. L. Martin and A. J. Sundermann, *J. Chem. Phys.*, 2001, **114**, 3408.
- 28 Basis sets were obtained from the Extensible Computational Chemistry Environment Basis Set Database, Version 6/19/03, as developed and distributed by the Molecular Science Computing Facility, Environmental and Molecular Sciences Laboratory which is part of the Pacific Northwest Laboratory, P.O. Box 999, Richland, Washington 99352, USA, and funded by the U.S. Department of Energy. The Pacific Northwest Laboratory is a multi-program laboratory operated by Battelle Memorial Institute for the U.S. Department of Energy under contract DE-AC06-76RLO 1830. Contact David Feller or Karen Schuchardt for further information.

- 29 A. D. Becke, *J. Chem. Phys.*, 1993, **98**, 5648.
- 30 C. T. Lee, W. T. Yang and R. G. Parr, *Phys. Rev. B*, 1988, **37**, 785.
- 31 J. A. Montgomery, M. J. Frisch, J. W. Ochterski and G. A. Petersson, *J. Chem. Phys.*, 1999, **110**, 2822.
- 32 R. A. Kendall, T. H. Dunning Jr. and R. J. Harrison, *J. Chem. Phys.*, 1992, **96**, 6796.
- 33 K. A. Peterson, D. Figgen, E. Goll, H. Stoll and M. Dolg, *J. Chem. Phys.*, 2003, **119**, 11099.
- 34 J. Gadhi, G. Wlodarczack, J. Legrand and J. Demaison, *Chem. Phys. Lett.*, 1989, **156**, 401.
- 35 E. A. C. Lucken, *Nuclear Quadrupole Coupling Constants*, Academic Press, London and New York, 1969.
- 36 A. Bauder, A. Beil, D. Luckhaus, F. Müller and M. Quack, *J. Chem. Phys.*, 1996, **106**, 7558.
- 37 Z. Kisiel, L. Pszczolkowsky, W. Caminati and P. G. Favero, *J. Chem. Phys.*, 1996, **105**, 1778.
- 38 T. Ueda and T. Shimanouchi, *J. Mol. Spectrosc.*, 1968, **28**, 350–372.
- 39 A. Cuisset, J. R. Aviles Moreno, T. R. Huet, D. Petitprez, J. Demaison and J. Crassous, *J. Phys. Chem. A*, 2005, **109**, 5708–5716.
- 40 D. Luckhaus and M. Quack, *Mol. Phys.*, 1989, **68**, 745–758.
- 41 J. Jacques, A. Collet and S. H. Wilen, *Enantiomers, Racemates and Resolutions*, J. Wiley & Sons, New York, 1981.
- 42 The presence of the two chlorine isotopes was also observed by ^{19}F NMR.
- 43 Octakis(3-*O*-butanoyl-2,6-di-*n*-pentyl)- γ -cyclodextrin linked via an octamethylene spacer to polydimethylsiloxane.
- 44 Z. Jiang, J. Crassous and V. Schurig, *Chirality*, 2005, **17**, 488–493.
- 45 For the synthesis of the racemic **7** by the direct method, see C. Garcia, D. Humilière, N. Riva, A. Collet and J.-P. Dutasta, *Org. Biomol. Chem.*, 2003, **1**, 2207–2216.
- 46 (a) C. Roussel, A. Del Rio, J. Pierrot-Sanders, P. Piras and N. Vanthuynne, *J. Chromatogr., A*, 2004, **1037**, 311–328; (b) C. Roussel, J. Pierrot-Sanders and I. Heitmann and P. Piras, in *Chiral Separation Techniques – A Practical Approach*, ed. G. Subramanian, Wiley-VCH, Weinheim, 2nd edn, 2001.
- 47 A. Tambuté, J. Canceill and A. Collet, *Bull. Chem. Soc. Jpn.*, 1989, **62**, 1390–1392.
- 48 L. A. Nafie and T. B. Freedman, in *Circular Dichroism: Principles and Applications*, ed. K. Nakanishi, N. Berova and R. Woody, Wiley-VCH, New York, 2nd edn, 2000, pp. 97–131.
- 49 T. B. Freedman, X. Cao, R. K. Dukor and L. A. Nafie, *Chirality*, 2003, **15**, 743–758.
- 50 P. L. Polavarapu and C. Zhao, *J. Anal. Chem.*, 2000, **366**, 727–734.
- 51 P. J. Stephens and F. J. Devlin, *Chirality*, 2000, **12**, 172–179.
- 52 S. J. Cianciosi, K. M. Spencer, T. B. Freedman, L. A. Nafie and J. E. Baldwin, *J. Am. Chem. Soc.*, 1989, **111**, 1913–1915.
- 53 S. J. Cianciosi, N. Ragunathan, T. B. Freedman, L. A. Nafie and J. E. Baldwin, *J. Am. Chem. Soc.*, 1990, **112**, 8204–8206.
- 54 T. B. Freedman, K. M. Spencer, N. Ragunathan, L. A. Nafie, J. A. Moore and J. M. Schwab, *Can. J. Chem.*, 1991, **69**, 1619–1629.
- 55 T. B. Freedman, S. J. Cianciosi, N. Ragunathan, J. E. Baldwin and L. A. Nafie, *J. Am. Chem. Soc.*, 1991, **113**, 8298–8305.
- 56 P. L. Polavarapu, *Chem. Phys. Lett.*, 1989, **161**, 485–489.
- 57 C. Garcia, C. Andraud and A. Collet, *Supramol. Chem.*, 1992, **1**, 31–45.
- 58 The faster running *anti* cryptophane *M*-(+)-**7** was accompanied with the slower running *syn* cryptophane which is achiral. For the *syn* and *anti* nomenclature in cryptophanes see A. Collet, J.-P. Dutasta, B. Lozach and J. Canceill, *Top. Curr. Chem.*, 1993, **165**, 103–129.
- 59 S. Kassi, D. Petitprez and G. Wlodarczak, *J. Mol. Struct.*, 2000, **517–518**, 375.
- 60 M. Goubet, P. Asselin, P. Soulard, M. Lewerenz and Z. Latajka, *J. Chem. Phys.*, 2004, **121**, 7784–7794.
- 61 L. A. Nafie, *Appl. Spectrosc.*, 2000, **54**, 1634–1645.
- 62 T. H. Dunning Jr. and P. J. Hay, in *Modern Theoretical Chemistry*, ed. H. F. Schaefer III, Plenum, New York, 1976, vol. 3, pp. 1–28.
- 63 P. J. Hay and W. R. Wadt, *J. Chem. Phys.*, 1985, **82**, 299–310.
- 64 W. R. Wadt and P. J. Hay, *J. Chem. Phys.*, 1985, **82**, 284–298.
- 65 W. J. Stevens, M. Krauss, H. Basch and P. G. Jasien, *Can. J. Chem.*, 1992, **70**, 612–630.
- 66 A. Bergner, M. Dolg, W. Kuechle, H. Stoll and H. Preuss, *Mol. Phys.*, 1993, **80**, 1431–1441.